Phase filed segmentation of high frequency 3D ultrasound images using log-likelihood

Khac Lan NGUYEN[1], Bruno SCIOLLA[2], Philippe DELACHARTRE[2], Michel BERTHIER[1]

[1]Laboratoire Mathmatiques, Images et Application
23 Avenue A. Einstein, BP 33060, 17031 La Rochelle, France

[2]Centre de Recherche en Acquisition et Traitement de l'image pour la Santé
7 Avenue Jean Capelle, 69621 Villeurbanne Cedex, France

khac.nguyen1@univ-lr.fr,
bruno.sciolla@creatis.insa-lyon.fr, philippe.delachartre@creatis.insa-lyon.fr,
michel.berthier@univ-lr.fr

Résumé – Nous nous intéressons dans ce travail au problème de la segmentation de tumeurs dans des images 3D Ultrasonores Hautes Fréquences. L'objectif principal est de présenter une méthode alternative à la méthode très largement utilisée, dite de Level Sets, introduite par Osher et Sethian. Pour cela, nous considérons un modèle de séparation de phases dont l'énergie, de Cahn-Hilliard, fait intervenir explicitement un potentiel à double puits. Cette énergie est bien connue pour être un bon modèle de transition dans des contextes physiques et chimiques variés de par le fait qu'elle prend en considération l'ensemble de la dynamique des processus d'évolution. L'énergie de Cahn Hilliard est couplée à une fonction de coût mesurant la dissimilarité des distributions d'intensité à l'intérieur et à l'extérieur de la tumeur (terme d'attache aux données). Les résultats obtenus montrent que cette approche est performante comparée à celle des Level Sets.

Abstract – We address in this work the problem of tumor segmentation in 3D High Frequeny Ultrasound images. The aim is to describe an alternative method to the widely used Level Set method introduced by Osher and Sethian. For this, we consider a separation phase model the energy of which, the Cahn Hilliard energy, involves a double well potentiel. This energy is well known to be a relevant transition model in various physical or chemical applications due to the fact that it takes into account the entire evolution process. The Cahn Hilliard energy is coupled with a cost function measuring the dissimilarity of intensity distributions inside and outside the tumor (data attachment term). Results show that this approach is relevant compared to the Level Set one.

1 Introduction

High frequency ultrasounds ($>$ 20 MHz) are a promising tool for diagnosis and surgery of skin tumors, for the cosmetic industry and for the imaging of organs in small animals. Ultrasound imaging uses the high-frequency sound waves to view inside the body. Ultrasound images are produced based on the reflection of the waves off of the body structures. This image acquisition mode is simple to deal with allowing frequent measurements and a good estimate of tumor growth. The acquisition process of ultrasound images is simple and take advantage of following the evolution of tumors. However, such images have two major intrinsic characteristics : their important noise (speckle) and their low and heterogenous contrast. Efficient segmentation of ultrasound images is designed relying on the local distribution of the signal envelope. Many successful approaches rely on the link between local scatterers properties and the statistics of the final ultrasound image envelope. It is generally assumed that the intensity distribution follows parametric distributions such as Rayleigh distributions [1], Rician distributions, K-distributions, Nakagami distributions [1, 2] or Fisher-Tippett distributions [7]. Unfortunately, all these approaches are limited to images displaying a broader variety of distributions. Worst still, heterogeneity can lead to more costly implementation, ill-founded approach or to considering bimodal distributions [3].

To tackle this problem, approaches involving non parametric distributions are introduced so as to divide the reference volume into two maximal distinct regions without any *a piori* assumption. Among others, let us mention methods using Parzen estimation and density dissimilarity measures such as Bhattacharyya distance, Kullback-Leibler divergence or log likelihood [14]. Due to the lack of contrast, 3D Ultrasound images do not exhibit strong contours. This explain why to use the well known Level Set method based on the statistics of the envelope signal in this context. An approach using both Level Sets and log likelihood has been recently applied for skin tumors segmentation in [3].

We propose here an alternative approach based on a coupling involving phase filed dynamic instead of Level Sets. We refer to [11, 12] for examples of application of the phase filed method to image segmentation. The main originality of this contribution is to evaluate the performance of this method dealing with High Frequency 3D Ultrasound images and to compare results with those obtained by Level Sets. It appears that our approach is simple for implementation and that its accuracy is comparable with the Level Set approach. The paper is organized as follows : we first describe the mathematical model, then we propose experiments on synthetic and clinical data.

2 Log-likelihood distance between intensity distributions

We rapidly describe the data attachment cost function that is coupled with the Cahn Hilliard energy. In the following, I_x denotes the intensity of the ultrasound image where x is the coordinates of the voxels. This is the normalized log-compressed envelope, which is the standard quantity used in the display of ultrasound images.During the segmentation process, the image volume is divided into the region of interest Ω_A and the background Ω_B with intensity distribution $P_A(I)$, $P_B(I)$. The log-likelihood distance is defined as :

$$LL = \sum_{x\in\Omega_A} \log \hat{P}_A(I_x) + \sum_{x\in\Omega_B} \log \hat{P}_B(I_x) \tag{1}$$

The distribution $P_A(I)$ in region Ω_A is estimated from the discrete set of voxel intensities $\{I(x),\ x \in \Omega_A\}$ using a Parzen estimation [13] :

$$\hat{P}_A(I) = \frac{1}{|\Omega_A|} \int_{\Omega_A} K_\lambda(I_x - I)dx \tag{2}$$

where $|\Omega_A|$ is the volume of Ω_A and the Kernel K_λ is chosen to be a normal distribution of width λ.

3 Phase field model

There exists a wide litterature concerning phase transition and phase boundary evolution models. These models find many applications in physics or chemistry. Among them, one of the most simple and well known in the image processing community is the so-called Level Set method, [4]. It is usually considered as a reference method. Besides this method, many other approaches can be considered. We deal in this work with the so-called phase filed method [5], and consider only isotropic deformation of the interface. The chosen Allen-Cahn reaction-diffusion equation reads :

$$\frac{\partial u}{\partial t} = \Delta u - \frac{1}{\epsilon^2} W'(u) \tag{3}$$

and can be derived as the L^2-gradient flow of the Cahn-Hilliard energy :

$$J_\epsilon(u) = \int_\Omega \left(\frac{|\nabla u|^2}{2} + \frac{1}{\epsilon^2} W(u) \right) dx \tag{4}$$

where the symbol u is used to denote the space time function $u(x,t)$ with t is the variable in time, W is double well potentiel and W' represents the derivative of W with respect to u. The symbol Δ is the Laplace operator. ϵ can be considered as the width of the transition interface. A classical choice for this potentiel is the polynomial $W(u) = u^2(1-u)^2/2$ the two global minima of which, 0 and 1, correspond to the two phases equilibria. The dynamic governed by the equation (3) can be interpreted as follows. At earlier times the reaction term given by the double well potentiel separates the two phases and creates rapidly a sharp interface or transition layer when $\epsilon \to 0$.Then the diffusion term given by the Lapalacian operator balances the action of the reaction term and stops the developpment of the interface. Pratically, the region of interest is defined by $\forall t \geq 0$, $\Omega_A = \{x : u(x,t) \geq 1/2\}$, the background region is defined by $\Omega_B = \{x : u(x,t) < 1/2\}$ and the transition layer, or active contour, or moving interface, is defined by $\Gamma_t = \{x : u(x,t) = 1/2\}$. One can prove, [6], that the energy (4) $\Gamma-$converges (when $\epsilon \to 0$) to $c_W P$ where $P(u) = \int_\Gamma \mathbf{1} d\sigma$ and $c_W = \int_0^1 W(s)ds$. This means that minimizing the Cahn-Hilliard energy is equivalent to minimizing the perimeter of the active contour.

4 Cahn-Hilliard log-likehood model

We set

$$E_\epsilon(u) = -LL(u) + \frac{\alpha}{c_W} J_\epsilon(u) \tag{5}$$

the cost function, minus the log-likelihood, being minimum when the distance between distributions is maximum. Note that this functional is non-convex, precluding the use of algorithms relying on this property. To minimize (5), we use the gradient flow descent $\partial_t u = -\frac{\delta E}{\delta u}$ that reads :

$$\begin{aligned} \partial_t u = 2u \log \hat{P}_A(I_x) + 2(u-1) \log \hat{P}_B(I_x) \\ + \frac{\alpha}{c_W} \left(\Delta u - \frac{1}{\epsilon^2} W'(u) \right) \end{aligned} \tag{6}$$

Using Lie splitting method, our numerical scheme is divided into three parts as shown by the algorithm 1. In this one, δt denotes the time step. U^n is the approximated value of $u(x, t^n)$ where $t^n = n\delta t$. U^0 is the initial condition. FFT and $IFFT$ denote respectively the Fast Fourier Transform and Inverse Fast Fourier Transform.

Algorithme 1

For : $n = 0, ...,$ convergence ($\|U^{n+1} - U^n\|_2 / \|U^n\|_2 \leq 10^{-6}$)

1. **DATA :** Entrance : U^0, δt, ϵ and I
2. Computation of the diffusion part : $\frac{\partial u}{\partial t} = \frac{\alpha}{c_W} \Delta u$

$$\begin{cases} U^n_{Fourier} = FFT[U^n] \\ U^{n+1/4}_{Fourier}[k] = e^{-4\alpha\pi^2|k|^2\delta t / c_W} U^n_{Fourier}[k] \\ U^{n+1/4} = IFFT[U^{n+1/4}_{Fourier}] \end{cases} \tag{7}$$

3. Computation of the data attachment part : $\frac{\partial u}{\partial t} = u \log \hat{P}_A(I) + (u-1) \log \hat{P}_B(I)$

$$\begin{aligned} U^{n+1/2} = U^{n+1/4} + \delta t U^{n+1/2} \log \hat{P}_A(I_x) + \\ \delta_t (U^{n+1/2} - 1) \log \hat{P}_B(I_x) \end{aligned} \tag{8}$$

4. Computation of the reaction part : $\frac{\partial u}{\partial t} = -\frac{\alpha}{c_W \epsilon^2} W'(u)$

$$U^{n+1} = U^{n+1/2} - \delta t \frac{\alpha}{\epsilon^2 c_W} W'(U^{n+1/2}) \qquad (9)$$

End for

The exact solution of the diffusion is computed by mean of FFT assuming periodic boundary conditions [8]. One can also deal with Dirichlet or Neumann conditions [5, 9]. Beside this easy to implement algorithm exist other possibilities leading to inconditionaly stable schemes : by replacing the reaction explicit scheme computing the exact solution or by using a hybrid FEM to solve the Allen-Cahn equation [10]. We choose here to use the simple to reproduce proposed algorithm dealing with FFT and the simple resolution of two ODEs (8) and (9).

Let us mention a major difference between Level Set and phase filed methods : from a methodological standpoint, the level set method is a computational approach in which the interface motion is numerically approximated using artificial smoothing function while the phase filed is based on a physical approach which incorporates the phases and the interface between them into the free energy function of the system. It means that the phase filed method not only transports the interface with the flow but ensures that the total energy of the system is minimized correctly. The evolution of the interface therefore is self-consistent in the phase filed method and does not need the re-initialization in the level set method. Moreover, in the phase field model one has to take care of the choice of the order parameter in order to control the interface motion. The proposed algorithm complies with the maximum principle for the heat equation. The Euler explicit scheme (9) comes with the stability condition $\delta_t < c_W \epsilon^2/\alpha$. The parameters α and ϵ are chosen to be respectively $O(\delta_x^2)$ and $O(\delta x)$ with δx the width of a spaced grid cell.

5 Test on synthetic and clinical 3D data

We propose first a quantitative test of our segmentation procedure using a synthetic ultrasound image. The image size in pixels is $216 \times 252 \times 168$. The target image is the red contour. The parameters are fixed as $\alpha = 8 \times 10^{-5}$, $\epsilon = \min(\delta x, \delta y, \delta z) = 0.004$, $\delta t = 0.8 c_W \epsilon^2/\alpha$, we take 100 values of $I \in [0, 1]$ for the Parzen estimation. The result of the segmentation is shown in figure 1. To quantify the precision of the segmentation results, the Dice coefficient and the mean absolute distance MAD are introduced. The Dice coefficient $D(\Omega, R)$ is computed for each segmented volume Ω with respect to the target volume R, i.e. $D(\Omega, R) = 2|\Omega \cap R|/(|\Omega| + |R|)$. We also compute the mean absolute distance MAD, which measures the accuracy of the boundary. For any voxel x in the boundary $\partial\Omega$ of Ω, we call $d^R(x)$ the distance of x to the closest point in R in pixels (1 pixel = 53 μm). $N_{\partial\Omega}$ is the number of voxels in the $\partial\Omega$. The mean distance is $MAD = \sum_{x \in \partial\Omega} d^R(x)/N_{\partial\Omega}$. For this synthetic example, we have $D(\Omega, R) = 0.8944$ and $MAD = 1.8752$ pixels. We note that the parameters ϵ, α, δt, even initial condition and its position may be changed if contrast of image is low. We evaluate now the performance of the proposed segmentation algorithm on a lesion image. The comparison is made using manual expert segmentation (reference 1 and 2). The skin tumor image has been acquired at the Melanoma Skin Cancer Clinic (Hamilton Hill, Australia) on a Dermcup 50MHz ultrasound imaging system (Atys Medical, Soucieu-En-Jarrest, France). The size in pixels of this ultrasound image is $832 \times 299 \times 300$ and the size of the region of interest in pixels is $454 \times 210 \times 242$.

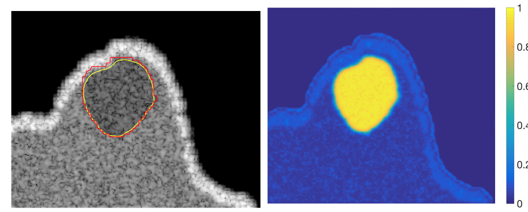

(a) (b)

FIGURE 1 – Slice of the segmented volume of the synthetic image : (a)Target volume (red) and segmented volume (yellow). (b) The phase separation.

For the experiment, we fixed $\delta z = 0.0022$, $\delta y = 0.0048$ and $\delta x = 0.0041$. As mentionned before, to obtain good results, it is necessary to adjust the order paremeter ϵ carrefully. Figure 2 shows the dependance of the Dice Index as a function of ϵ, the parameter α being fixed $\alpha = 6 \times 10^{-5} = O((\delta z)^2)$ and $\delta t = 0.8 c_W \epsilon^2/\alpha$. The figure 2 shows the optimal value of ϵ : $\epsilon = 0.0022$. For the very small values of ϵ ($\epsilon < 0.022$), the active contour do not move. While the big values of ϵ ($\epsilon > 0.0022$) make the segmented volume inaccurate. Figure 3 shows the segmented volume and the segmented contour compared to the two references. Tables 1 and 2 show the comparison of the results obtained by the Level Set method [3] and by the phase filed approach.The parameters are chosen to maximize the Dice coefficient for each method. In these tables R_{m1} and R_{m2} denote the manual expert references. We observe that the Dice coefficient for both methods is similar and that it is slightly better for the phase filed approach. We observe also that the MAD coefficient is better for the proposed method.

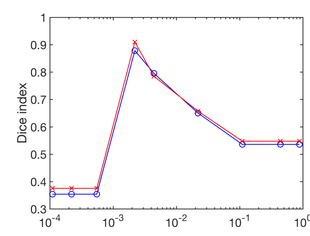

FIGURE 2 – Dice Index as a function of ϵ with fixed $\alpha = 6 \times 10^{-5}$ (blue, reference 1 - red, reference 2)

The Cahn-Hilliard log-likehood model reveals to be an accurate tool for the segmentation of ultrasound image of clinical data. The simple implementation we propose, based on Eu-

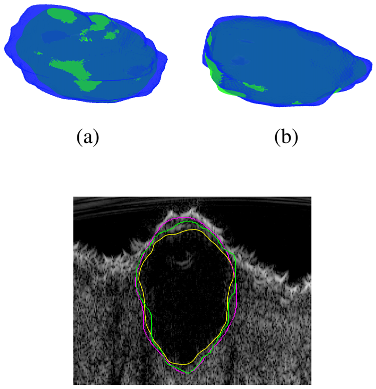

(a) (b)

(c)

FIGURE 3 – (a) Segmented volume (green) with the volume of reference 1 (blue). (b) Segmented volume (green) with the volume of reference 2 (blue). (c) Slice : the segmented contour (yellow), the contour of reference 1 (pink) and the contour of reference 2 (green)

TABLE 1 – Dice coefficient : Level set and phase filed

Coefficient	$D(\Omega, R_{m1})$	$D(\Omega, R_{m2})$
Level set	0.8500	0.8798
Phase filed	0.8786	0.9100

TABLE 2 – MAD (in pixels) : Level set and phased filed

Coefficient	$MAD(\partial\Omega, \partial R_{m1})$	$MAD(\partial\Omega, \partial R_{m2})$
Level set	4.6642	3.7974
Phase filed	3.8145	2.8652

ler explicite and implicite scheme and using the first order Lie splitting is, as we have mentioned before, not optimized and takes time to deal with big data such as 3D ultrasound images containing millions of voxels.

6 Conclusion

We proposed in this work a new method for 3D Ultrasound images segmentation. Our approach is based on a phase field model using a regularization term coming from the Cahn-Hilliard energy and a data attachment term taking into account the dissimilarity of pixel distributions. It provides a good alternative to the well known Level Set method and shows results on clinical data slightly better than this latter. There exist many possibilities to improve to speed of the method : by using hybrid FEM schemes, by replacing the schemes by the exact solutions of the reaction part and the data attachment part or by using Multi-grid method. There exist also many possibilities to extend the proposed approach by mean of more sophisticated phase field models taking into account anisotropy or surface tension for instance.

Références

[1] F. Destrempes, G. Cloutier, *A critical review and uniformized representation of statistical distributions modeling the ultrasound echo envelope*, Ultrasound in Medicine and Biology, vol. 36, no. 7, pp. 1037-1051, 2010.

[2] J. Anquez, E. Angelini, G. Grange, I. Bloch, *Automatic segmentation of antenatal 3-d ultrasound images*, Biomedical Engineering, IEEE Transactions on, vol. 60, no. 5, pp. 1388-1400, May 2013.

[3] B. Sciolla, L. Cowell, T. Dambry, B. Guibert, B. Delachartre, *Segmentation of Skin Tumors in High-Frequency 3-D Ultrasound Images*, Ultrasound in Medicine & Biology, vol. 45, no. 1, pp. 227-238, January 2017.

[4] J. A. Sethian, *Theory, Algorithms, and Applications of Level Set Methods for propagating Interfaces*, Acta Numerica, 1995.

[5] E. Bretin, *Mouvement par courbure moyenne et methode de champ de phase*, Ph.D. thesis, Institut polytechnique de Grenoble (2009).

[6] L. Modica, S. Mortola *Un esempio di gamma-convergenza*, Boll. Un. Math. Ital. vol. 14, no. 1, pp. 285-299, 1977.

[7] G. Slabaugh, G. Unal, T. Fang, M. Wels, *Ultrasound-Specific Segmentation via Decorrelation and Statistical Region-Based Active Contours*, Computer Vision and Pattern Recognition, 2006 IEEE Computer society Conference on, pp. 1063-6919, July 2006.

[8] L. Q. Chen, J. Shen, *Applications of semi-implicit fourier-spectral method to phase filed equations*, Computer Physics Communications, Vol. 108, pp. 147-158, 1998.

[9] A. Wiegmann, *Fast elliptic solvers on rectangular parallelepipeds*, Technical report, LBNL Technical Report, 1999.

[10] J. Shin, S.K. Park, J. Kim, *A hybrid FEM for solving the Allen-Cahn equation*, Applied Mathematics and Computation, vol. 244, pp. 606-612, 2014.

[11] S. Esedoglu, Y. H. R. Tsai, *Threshold dynamics for the piecewise constant mumford-shah functional*, Journal of Computational Physics, vol. 211, pp. 367-384, 2006.

[12] S. Zhao, M. Zhou, T. Jia, P. Xu, Z. Wu, Y. Tian, Y. Peng, S. J. Jin, *Multi-branched cerebrovascular segmentation based on phase-field and likelihood model*, Computers & Graphics, vol. 38, pp. 239-247, 2014.

[13] E. Parzen, *On Esitmation of a Probability Density Function and Mode*, Annals of Math. statistics, vol. 33, Issue 3, pp. 1065-1076, Sep. 1962

[14] B. Sciolla, P. Ceccato, T. Dambry, B. Guibert, P. Delachartre *A comparison of non-parametric segmentation methods*, Colloque GRETSI 2015, Sep 2015, Lyon, France. Actes du colloque GRETSI 2015 pp. 4, http ://gretsi.fr/colloque2015/